Journal of Applied Electrochemistry
https://doi.org/10.1007/s10800-019-01394-z

RESEARCH ARTICLE

Performance of H_2-fed fuel cell with chitosan/silicotungstic acid membrane as proton conductor

Francesco Di Franco[1] · Andrea Zaffora[1] · Giuseppe Burgio[1] · Monica Santamaria[1]

Received: 9 July 2019 / Accepted: 31 December 2019
© Springer Nature B.V. 2020

Abstract

Composite organic–inorganic proton exchange membranes for H_2–O_2 fuel cells were fabricated by ionotropic gelation process combining a biopolymer (chitosan) with a heteropolyacid (silicotungstic acid). According to scanning electron microscopy analysis, compact, homogeneous and free-standing thin layers were synthesized. X-ray diffraction proved the crystallinity of the fabricated membranes and showed the presence of Chitosan Form I polymorph soon after the reticulation step and of the Form II polymorph after the functionalization step. Fourier-transform infrared spectroscopy demonstrated that the Keggin structure of the heteropolyacid is maintained inside the membrane even after the fabrication process. These membranes worked properly as proton conductors in a low-temperature (25 °C) fuel cell apparatus using hydrogen as fuel recording a promising power density peak of 268 mW cm^{-2} with a Pt loading of 0.5 mg cm^{-2}.

Graphic abstract

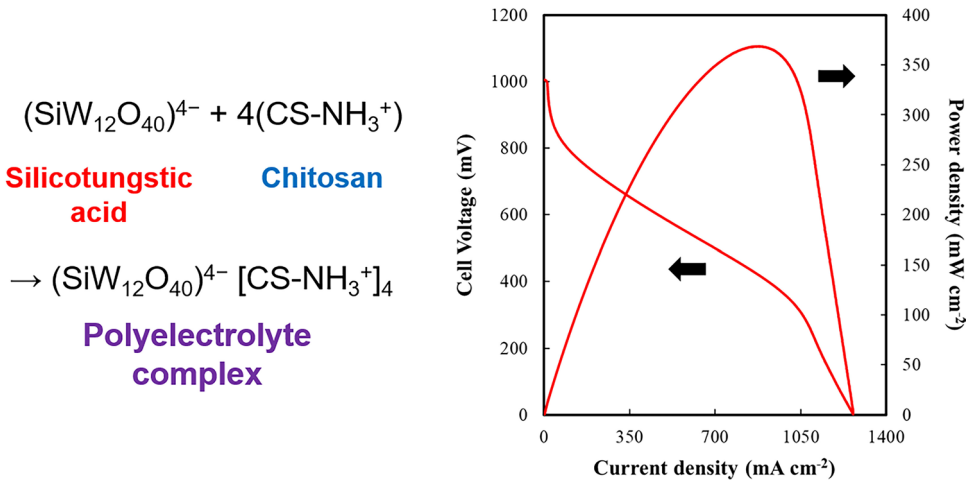

Keywords Chitosan · Silicotungstic acid · Composite membrane · H_2–O_2 PEMFC

1 Introduction

Proton exchange membrane fuel cells (PEMFCs) are among the most promising energy conversion devices due to their high power density, high efficiency, environmental friendliness and fast startup and shutdown [1, 2]. Surely, the solid electrolyte (i.e. the membrane) is the key component in these electrochemical devices due to the critical

✉ Andrea Zaffora
andrea.zaffora@unipa.it

[1] Dipartimento di Ingegneria, Università degli Studi di Palermo, Viale delle Scienze, Ed. 6, 90128 Palermo, Italy

Published online: 21 January 2020

role in conducting protons from anodic to cathodic compartment and in avoiding direct gases reaction and short circuits. To date, Nafion® membrane is the benchmark due to its high proton conductivity, physical and chemical stability [3–5]. However, Nafion® needs quite high temperature to provide high proton conductivity; its high thickness leads to an increase in the resistance for proton transport and, finally, it is expensive.

Different approaches have been followed to develop reliable substitutes of Nafion®, including the synthesis of composite membranes, e.g. composite organic–inorganic solid electrolytes that could enable higher or lower operating temperatures with comparable or better performances [6, 7]. In this context, a polymer used in composite membranes with Nafion® is Chitosan (CS) [8] that is derived from chitin (the second most present natural polymer in the world [9]) through a *N*-deacetylation process.

CS can be considered promising in the attempt to find a cheap and low environmental impact alternative to perfluorosulfonic acid membranes, even if this biopolymer has a low proton conductivity and low thermal stability. Increasing membrane proton conductivity can be obtained using heteropolyacids (HPAs), transition metal oxide clusters that can have several structural configurations and have high H^+ conductivity. Indeed, they act as strong Brønsted acids and can keep a pseudo-liquid phase even at relatively high temperature [10]. HPAs usually assume a crystalline form and are highly soluble in water; thus they cannot be used directly as solid electrolyte. Protonated chitosan chains, i.e. cationic polyelectrolytes, can therefore react with anions derived from heteropolyacid to prepare polyelectrolyte complexes (PECs), which are usually water insoluble, to be employed as proton conductors.

As reported in previous works [11–14], composite CS/HPA membranes can be successfully prepared using an alumina porous medium for the slow and uniform release of the heteropolyacid, showing good performances as solid electrolytes in PEMFCs fed with hydrogen and oxygen at room temperature. In particular, membranes prepared with phosphotungstic acid showed very promising performances [11–13] with a power density peak of ~ 550 mW cm^{-2}. In order to further enhance the fuel cell performances, addenda atom of the heteropolyacid was changed (Mo^{6+} instead of W^{6+}), leading anyway to worse results [14]. Changing heteroatom of the acid (Si instead of P) could be the strategy to get better results in terms of electrode kinetics and membrane durability. In fact, according to the literature, hybrid polymer-silicotungstic acid (STA) membranes have a high thermal stability, promising mechanical strength and proton conductivity [10, 15–18]. Moreover, the addition of STA to the electrodes of polymer electrolyte membranes fuel cells is reported to enhance the activity of platinum towards oxygen reduction reaction and the stability of the membrane [19–21].

In this work, we investigated the potential of composite chitosan/silicotungstic membranes as polymer electrolyte in PEMFCs operating at low temperature and fed with hydrogen. The characterization of these membranes, synthesized by ionotropic gelation, has been carried out by using scanning electron microscopy (SEM) to study their morphology, and X-ray diffraction (XRD) and Fourier-transform infrared (FTIR) Spectroscopy in order to study their structure and composition. Polarization curves were recorded to evaluate their performance in a single-module H_2-fed fuel cell, whilst electrochemical impedance spectroscopy (EIS) was employed to model the kinetic of the cell reaction and to estimate the membrane proton conductivity.

2 Experimental

Membranes were synthesized by ionotropic gelation process as described elsewhere [13]: a chitosan (CS)/acetic acid aqueous solution and a porous anodic alumina film impregnated with silicotungstic acid ($H_4[Si(W_3O_{10})_4]\cdot xH_2O$, STA) were put in contact for the reticulation step in which cross-linking reaction occurs with membrane thickening (ionotropic gelation process). A membrane functionalization step was performed by immersing the obtained membrane in the STA-water solution (1:1 w/w) in order to increase the heteropolyacid content in the ion-exchange membrane, i.e. to increase the membrane proton conductivity. Different reticulation and functionalization times led to different thicknesses (see below).

Membranes morphology and thickness were studied through scanning electron microscopy (SEM) analysis, using a Philips XL30 ESEM (working at 10 kV) coupled with energy dispersive X-ray (EDX) equipment. XRD patterns were obtained with a X-ray diffractometer (Pan Analytical Empyrean), equipped with a Cu anode (Kα radiation, $\lambda = 0.15405$ nm, operating voltage: 40 kV, operating current: 40 mA). Fourier-transform infrared (FTIR) spectra of the specimens were examined on a FTIR spectrometer (PerkinElmer Spectrum Two) in ATR mode between 400 and 4000 cm^{-1} as wavenumber.

Home-made electrodes for fuel cell testing were fabricated following two different methods [13]: (a) the catalyst suspension was made of 1.1 g of Pt/C (30%wt. of Pt on Vulcan XC e 72, E-Tek) and 50 ml of *n*-butyl acetate (99.7% Sigma Aldrich). 2 ml of the suspension were then uniformly dispersed on 12.56 cm^2 of carbon paper (Toray 40% wet Proofed-E-Tek) and then left drying for at least 12 h. In this case, Pt loading was 1 mg cm^{-2} for both the anode and the cathode sides (s-CL); (b) a catalytic ink was sprayed on a Sigracet—24BC gas diffusion layer [22]. The catalytic ink

was made by mixing the 50%wt. Pt/C (Alfa Aesar) with a 33%wt. of dry Nafion (5%wt. hydro-alcoholic solution, Ion-Power e LQ1105) with an equivalent weight of 1100 g/mol. Then, 20%wt. of ammonium carbonate (Carlo Erba) was used as a pore former for the preparation of the catalyst layer. Pt loading was fixed at 0.5 mg cm^{-2} for both the anodic and the cathodic reactions (i-CL).

The electrodes and the membrane constituted the Membrane Electrode Assembly (MEA) that was then used in a fuel cell (Electrochem Inc.), with an applied torque to the apparatus of 2 Nm. Hydrogen (99.5% purity) and oxygen (99.5% purity) were fed to the system at 1 bar and room temperature (25 °C).

Open circuit voltage (OCV) was measured before any electrochemical measurements until it reached a steady value. Cell voltage vs. current density curves have been recorded starting from OCV value to short circuit condition (0 V) at a scan rate of 100 mV s^{-1}. Electrochemical Impedance Spectra were carried out by superimposing to the constant continuous voltage, a sinusoidal signal, of amplitude 10 mV over the frequency range 10 kHz–100 mHz. All electrochemical measurements were carried out by using a Parstat 4000 (Princeton Applied Research) and the results of EIS spectra were then fitted with ZSimpWin software. The active (apparent) area was 2 cm^2.

A sketch of the experimental setup and of fuel cell assembly is shown in Fig. 1.

3 Results and discussion

3.1 SEM analysis

Composite proton exchange membranes are produced through the following reaction:

$$\left(SiW_{12}O_{40}\right)^{4-} + 4\left(CS - NH_3^+\right) \rightarrow \left(SiW_{12}O_{40}\right)^{4-}\left[CS - NH_3^+\right]_4 \quad (1)$$

i.e. protonated NH_2 groups of chitosan interact with $(SiW_{12}O_{40})^{4-}$ polyoxometalate anions, released by STA impregnated porous alumina film, leading to an ionic cross-linking and, thus, to the membrane thickening. In order to study how the reticulation and the functionalization steps influence the morphology and the thickness of the membranes, SEM analysis was carried out. Figure 2 shows SEM micrographs relating to the cross section of CS/STA membranes prepared at different reticulation time: 0.5 min (see Fig. 2a) and 30 min (see Fig. 2b).

The films are homogeneous and compact, regardless of reticulation or functionalization times (t_{ret} and t_{fun}, respectively), as reported for analogous composite membranes prepared with CS and phosphotungstic acid [12, 13]. This result is the consequence of a uniform cross-linking process of the STA^{4-} ions along the chitosan chains directly related to the fabrication method. Membranes thickness, d_{el}, was estimated taking into account the average values between those measured in five points of at least three membrane samples fabricated following the same preparation conditions. A fast increase of the membrane thickness is detected for low reticulation times, between 10 µm for 0.5 min reticulated films and 20 µm for 10 min reticulated films, whilst a linear increase occurs for $t_{ret} \geq 10$ min. Thickness values increase

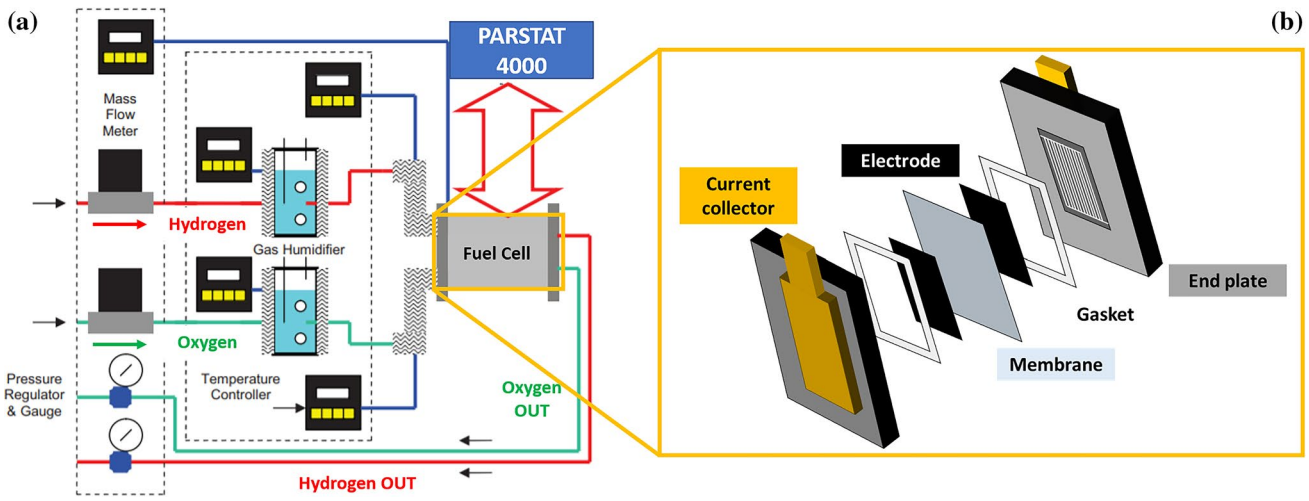

Fig. 1 **a** Sketch of the experimental setup and **b** fuel cell assembly

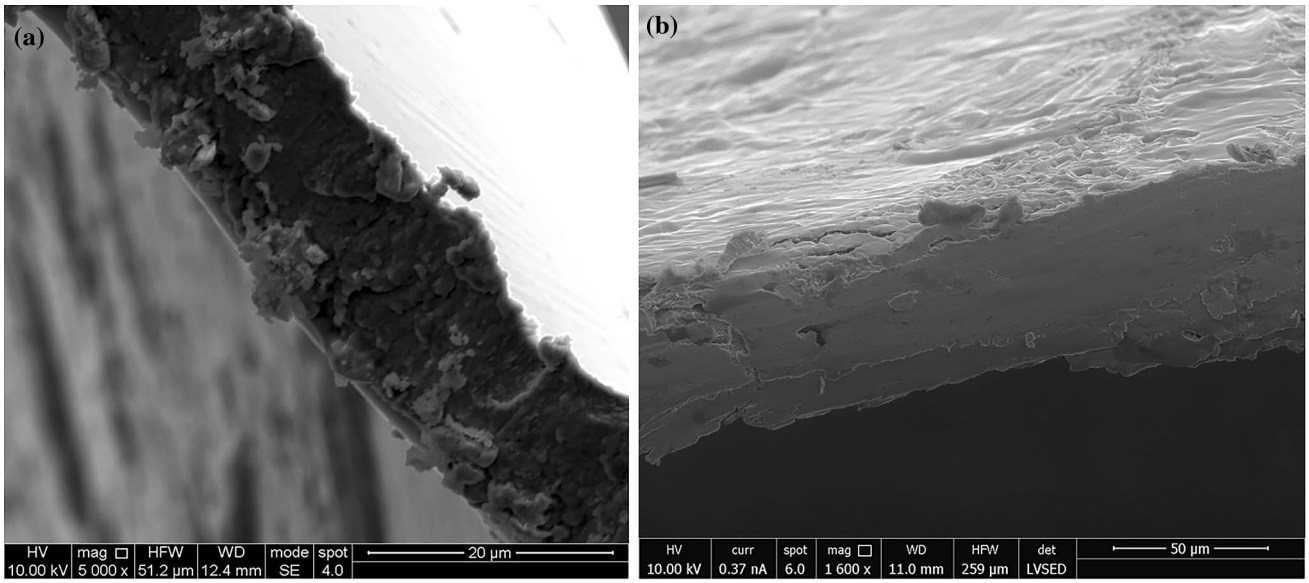

Fig. 2 SEM micrographs of CS/STA membranes. Reticulation times: **a** 0.5 min, **b** 30 min. Functionalization time: 24 h

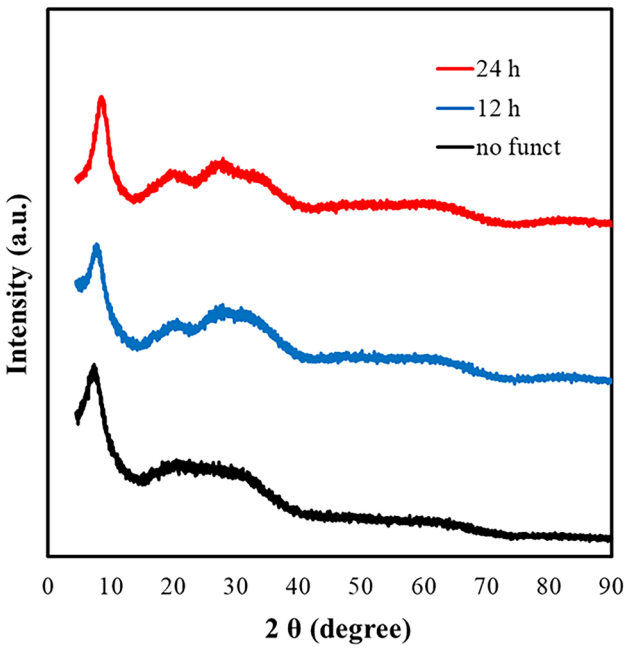

Fig. 3 X-ray diffraction patterns relating to CS/STA membranes reticulated for 0.5 min with several functionalization times

of ~ 2 times if the membranes undergo the 24 h functionalization step, whatever is the reticulation time, varying between 16 and 59 µm.

3.2 X-ray diffraction and FTIR spectroscopy

Figure 3 shows X-ray diffraction patterns relating to CS/STA membranes: as prepared, after a 12 h functionalization step in STA and after 24 h of functionalization in STA solution. According to the literature [23, 24], six Chitosan polymorphs can be recognized: tendon, annealed, '1–2', 'L-2', 'Form I' and 'Form II'. The diffraction patterns of CS/STA membranes show the presence of a main peak at $2\theta = 7.5°$ (related to the Form I polymorph), whilst other two peaks become evident after the membrane functionalization at $2\theta = 20.5°$ and 28.3° (related to the Form II polymorph). This increase in the crystallinity degree of the CS/STA membranes can be explained by considering the structure of CS polymer and what happens during all the fabrication steps. As reported in literature [25], intra- and intermolecular hydrogen bonds stabilize the crystalline structure of pure CS. Anyway, the hydrogen bonds between the NH_2 groups of glucosamine repeating units of CS are disrupted when CS is protonated, i.e. when it reacts with acetic acid and during the reticulation step. This phenomenon leads to the weakening of the rigid structure, as shown in the membrane diffraction pattern of Fig. 3 (black line). However, the functionalization step induces a more ordered membrane structure with a reduction of the reticulation degree (i.e. in the chains packing) because of the interaction between the CS/STA layers and the silicotungstic solution employed for the functionalization. During the latter step, it is supposed that STA^{4-} ions (that are ionically bonded with four protonated NH_2 groups) can take protons from fresh $H_4SiW_{12}O_{40}$, with a following decrease in the chains packing and the consequent availability of H bonded to the Keggin ions with the increase of proton conductivity.

FTIR spectra of CS/STA membranes are reported in Fig. 4 as a function of reticulation and functionalization times (0 min in Fig. 4a) and 24 h in Fig. 4b). Pure STA

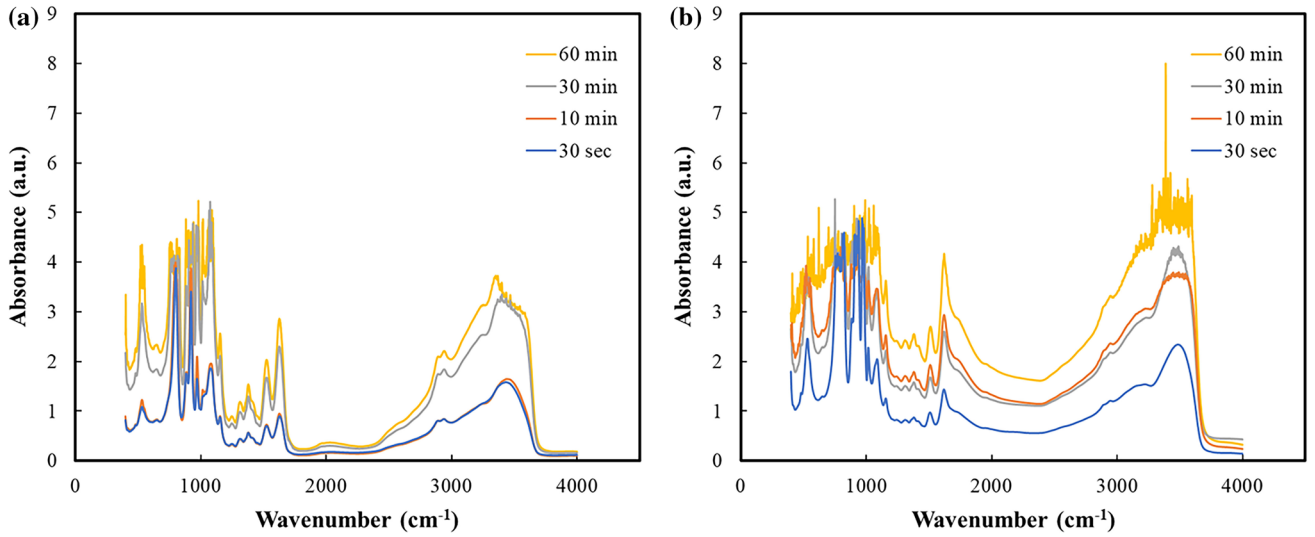

Fig. 4 FTIR spectra of CS/STA membranes as a function of reticulation time with **a** no functionalization step and **b** 24 h functionalization

spectrum presents five absorption characteristic bands, relating to the Keggin structure: 1018 cm^{-1} (Si–O), 975 cm^{-1} (W–O–W), 926 cm^{-1} (Si–O), 912 cm^{-1} (Si–O–W), 879 cm^{-1} (W–O_b–W) and 786 cm^{-1} (W–O_c–W) [15, 26, 27]. These bands appear also in the FTIR spectra of the CS/STA complex structures, so that the Keggin structure of the heteropolyacid is preserved even after the ionotropic gelation fabrication process. Besides STA characteristics, also CS bands are present in the spectra relating to the membranes; in particular, the bands at 1382 cm^{-1} (related to the –CH_3 symmetric deformation of CS) at 1531 cm^{-1} and at 1630 cm^{-1} (related to the NH_3^+ bending vibrations) are present, whilst the characteristic band of –NH_2 bending vibrations (1587 cm^{-1}) is not present. These results lead to the conclusion that the –NH_2 groups of the glucosamine units of CS in CS/STA membranes are protonated during the dissolution of CS in the water/acetic acid solution and by STA^{4-} ions during the reticulation step, confirming the presence of ionic bonds between CS and Keggin (polyoxometalate) anions. Furthermore, the band starting from 3200 cm^{-1} is related to the stretching vibration of N^+–H. This is probably sensitive to the presence of STA^{4-} anions, because of the strong interaction between the latter and NH_3^+ groups by ionic bonding. Such band continued to broaden by increasing the time of the reticulation step: this result can be explained considering that much more STA^{4-} ions interacted with the NH_3^+ [28].

3.3 Fuel cell performances and EIS study

CS/STA membranes were used as proton conducting membranes in H_2–O_2 based fuel cells, operating at room temperature (25 °C) employing a membrane reticulated for 0.5 min and functionalized for different times in STA aqueous solution with a low Pt load at both the electrodes (i.e. 0.5 mg cm^{-2}). OCV reaches 0.86 V, i.e. a lower value than cell electromotive force, *emf* (1.23 V), primarily due to the H_2 crossover to the cathodic compartment, but close to the OCV value reported for H_2–O_2 fuel cells employing CS/HPA-based membranes [12].

In Fig. 5, the polarization curve and power density vs current density curve recorded during fuel cell operation, as a function of the functionalization time, are reported. It is

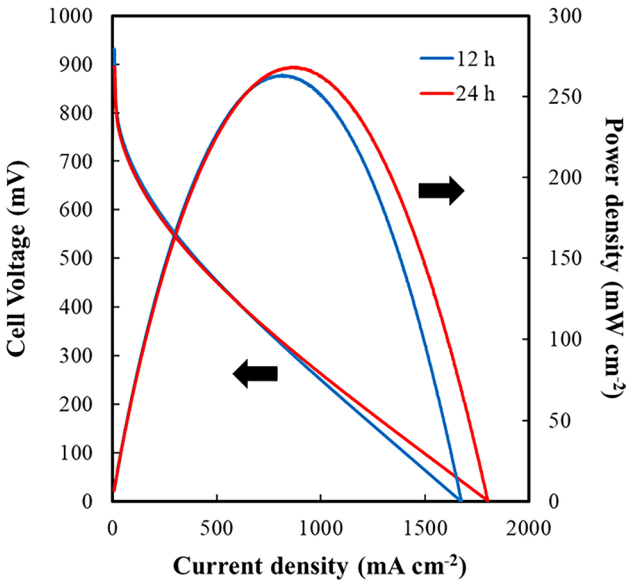

Fig. 5 Polarization and power density curves related to CS/STA membranes reticulated for 0.5 min with different functionalization times

noteworthy to mention that employing membrane not previously functionalized in STA aqueous solution led to devices not able to generate electrical energy. This finding suggests that functionalization is a key step to enable the proton conduction in composite CS/HPA membranes. During fuel cell test, OCV value is higher than that reported above since the membrane humidifies during the operation. It is clearly possible to distinguish two different zones in the polarization curve: the activation region (between OCV and ~ 0.6 V), where the rate determining step is the charge transfer, and the ohmic region, where the voltage drop is essentially due to the resistance of the membrane. From the slope of the polarization curve in the linear region, it has been estimated the resistance of the membrane (electrolyte), R_{el}, as 0.37 Ω cm^2 and 0.33 Ω cm^2, for 12 h and 24 h as functionalization time, respectively. These resistance values are higher than those related to CS/PTA membranes [13] and lower with respect to those estimated for CS/phosphomolybdic acid (PMA) membranes [14]. It is worth noting that the values of R_{el} are comparable to those reported for Nafion 211® employed as polymer electrolyte in H_2-fed fuel cell [29]. Thus, the proton conductivity, σ, can be estimated as follows:

$$\sigma = \frac{d_{el}}{A}\frac{1}{R_{el}} \tag{2}$$

where A is the active area of the membrane. Proton conductivities of 3.50 and 4.88 mS cm^{-1} were estimated. Moreover, knowing R_{el} it is possible to estimate the cathodic reaction overvoltage, η_C, and thus to make some consideration about the kinetics of the O_2 reduction. In fact, η_C can be calculated according to the following relationship:

$$|\eta_C| = emf - E_{cell} - iR_{el} - \eta_A \tag{3}$$

where E_{cell} is the cell potential and η_A is the anodic reaction overvoltage, considered negligible since the H_2 oxidation reaction at Pt electrode has fast kinetics. The Tafel plots, i.e. $|\eta_C|$ vs $\log_{10}(i)$ curves, are reported in Fig. 6. The slope of the linear region of the Tafel plots is ~ 120 mV per decade in the case of 12 h functionalized membrane and 130 mV per decade for 24 h functionalized membrane. These slope values are comparable to the typical value reported when the oxygen reduction process is under charge transfer control [30]. Exchange current densities, i_0, for the O_2 reduction reaction of 8 μA cm^{-2} (assuming the geometrical surface) for the former membrane and 12 μA cm^{-2} for the latter can be estimated from the *y*-axis intercept of the fitting lines, slightly higher than that estimated in the same experimental conditions using CS/PTA composite membranes [13]. This finding suggests the formation of an efficient electrode/polymer electrolyte interface with good activity towards O_2 reduction.

The power density peak was reached by using the membrane functionalized for 24 h; the maximum was showed in the ohmic region of the polarization curve and was 268 mW cm^{-2} @ $i = 880$ mA cm^{-2} and $E_{cell} = 306$ mV. This result is remarkable since it is better than other results reported in literature for systems employing STA-based membranes [31]. It is noteworthy to mention that, despite the high current densities, the polarization curve still had ohmic behaviour without any signal of mass transfer-controlled kinetics or cell flooding, which was reported for other H_2–O_2 fuel cell employing heteropolyacid-based solid electrolyte [11].

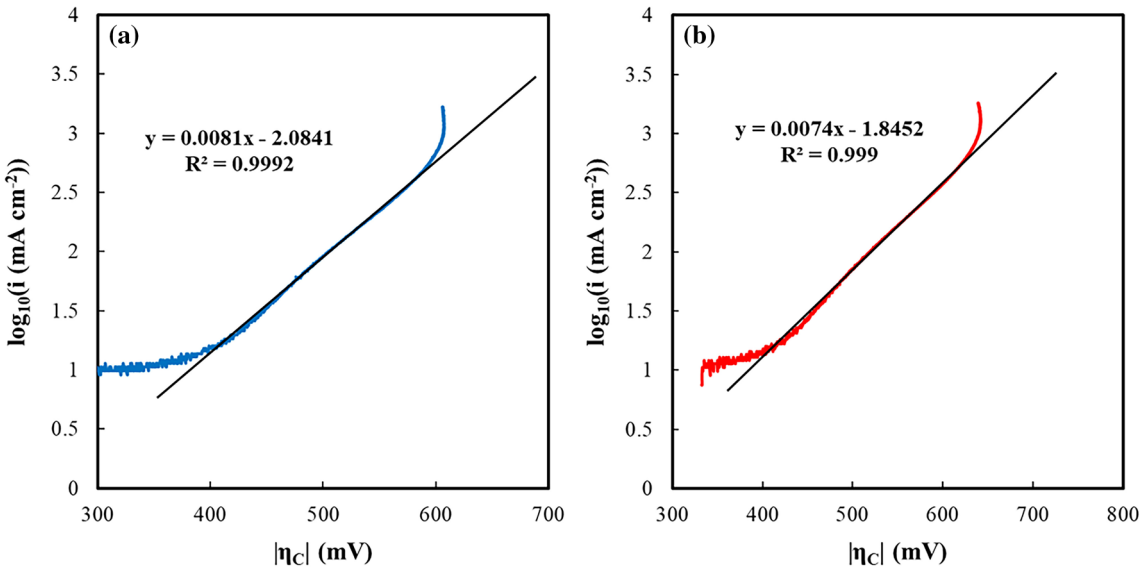

Fig. 6 Tafel plots derived from polarization curves of Fig. 4. Functionalization time: **a** 12 h, **b** 24 h

The behaviour of the STA-based membrane fuel cell was further investigated by EIS measurements, recorded both in activation region (E_{cell} = 750 mV) and in ohmic region (E_{cell} = 450 mV). The corresponding Nyquist plots are reported in Fig. 7 (functionalization time: 12 h (see Fig. 7a) and 24 h (see Fig. 7b)). EIS spectra were therefore simulated with the equivalent electrical circuit shown in the inset of Fig. 7a [13]: the parallel between R_C and Q_C is used to model the charge transfer resistance and double-layer capacitance at the cathodic side, as well as the parallel between R_A and Q_A accounts for the electrochemical behaviour of the anode.

The parameters derived to be the best fitting procedure are reported in Table 1. Firstly, R_{el} resulted slightly lower than that estimated from the linear part of the polarization curve, probably due to the higher hydration level of the membrane during the EIS measurement and, thus, a higher proton conductivity that strongly depends on the hydration level of the solid electrolyte. Noteworthy, the contribution to the overall cell impedance coming from the H_2 oxidation reaction, revealed by the very low R_A value, resulted to be almost negligible due to the very high catalytic activity of Pt toward such reaction. R_C, one order of magnitude higher with respect to R_A, accounts for the sluggish kinetics of the oxygen reduction reaction. As expected, the contributions of the kinetics to the overall cell impedance are almost normalized in the ohmic region where R_A and R_C have comparable values.

An increase in the Pt loading (1 mg cm^{-2}) allowed to obtain even better performance (power density peak of 370 mW cm^{-2}) as shown in Fig. 8 where the polarization and power density curves are reported. Notably, the OCV value is higher with respect to those recorded and shown in Fig. 5 for MEAs with a Pt loading of 0.5 mg cm^{-2} (i-CL) due to the lower activation losses for O_2 reduction and crossed H_2 oxidation at open circuit. It is important to stress that the OCV value recorded with this CS/STA membrane is even higher than that recorded, in the same configuration, with composite CS/PTA membrane [13], suggesting a lower H_2 permeability through the CS/STA membrane. Remarkably, at current density higher than 1000 mA cm^{-2}, it is evident the starting of the diffusion controlled region with a decrease of the slope of polarization curve by increasing the current density. As reported by Santamaria et al. [13], this phenomenon can be clarified considering the H_2O accumulation and pore filling at the cathode gas diffusion layer (GDL) due to the employed catalyst. Furthermore, we tested

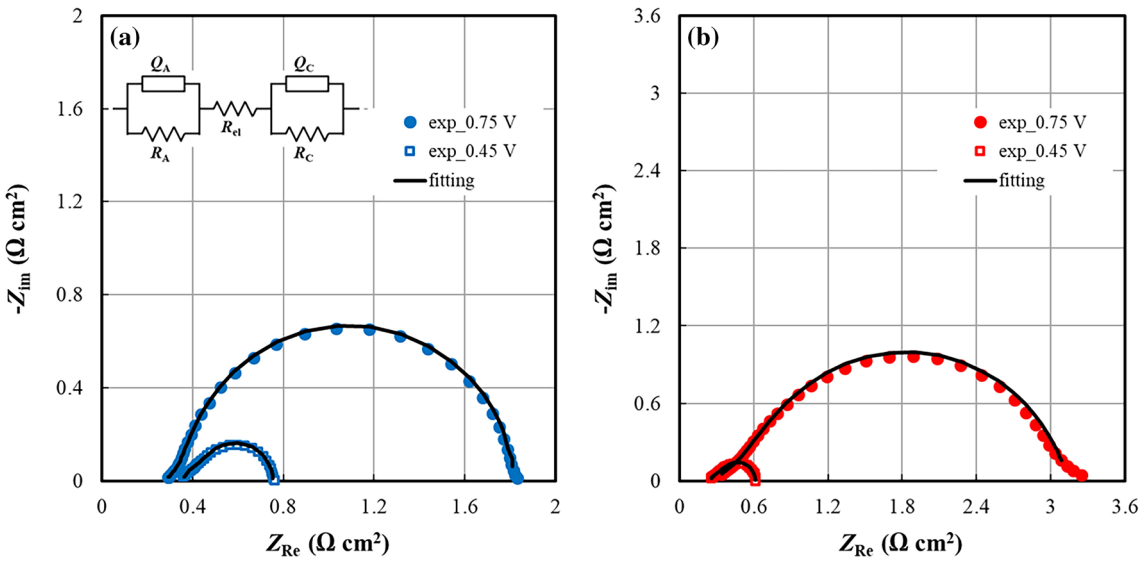

Fig. 7 Nyquist plots of EIS spectra recorded at (filled circle) 0.75 V and (square) 0.45 V related to CS/STA membranes reticulated for 0.5 min and functionalized for **a** 12 h and **b** 24 h. Inset: equivalent electrical circuit used for EIS data fitting

Table 1 Fitting parameters related to EIS spectra shown in Fig. 7

t_{fun} (h)	E_{cell} (V)	R_{el} (Ω cm^2)	R_A (Ω cm^2)	Q_A (S s^n cm^{-2})	n	R_C (Ω cm^2)	Q_C (S s^n cm^{-2})	n
12	0.75	0.28	0.09	7.8×10^{-3}	0.94	1.45	6.0×10^{-2}	0.60
	0.45	0.35	0.11	5.5×10^{-3}	1	0.30	1.2×10^{-2}	0.76
24	0.75	0.34	0.27	1.0×10^{-2}	0.84	2.46	6.7×10^{-2}	0.46
	0.45	0.25	0.12	5.6×10^{-3}	1	0.25	1.5×10^{-2}	0.71

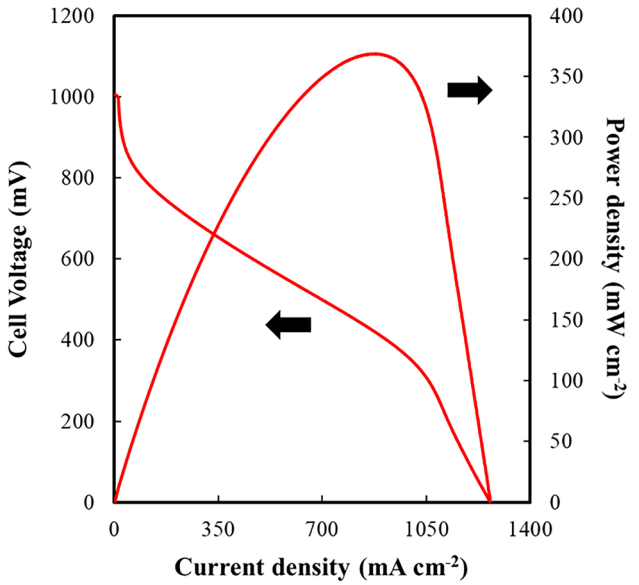

Fig. 8 Polarization and power density curves related to CS/STA membranes reticulated for 0.5 min and functionalized for 24 h with 1 mg cm^{-2} as Pt loading at the electrodes

the stability of the membrane by applying a constant E_{cell} of 0.5 V for ~ 7000 s. After cell shut down and restart, we recorded polarization and power density curves confirming the performances of Fig. 8, thus proving the stability of the CS/STA membrane proton conductor in the MEA.

4 Conclusion

Composite Chitosan/Silicotungstic acid membranes were synthesized and employed as solid electrolyte in H_2-based low-temperature fuel cells. Thin layers growth was carried out through ionotropic gelation process using a porous anodic alumina medium to control the release of the silicotungstic acid allowing for preparing free-standing and compact membranes. SEM analysis evidenced the formation of homogeneous polymer (without the presence of flaws or macrovoids), whose thickness strongly depends on reticulation time and slightly change after the functionalization step. X-ray diffraction and FTIR confirmed that membranes are scarcely crystalline soon after reticulation but become more ordered as a consequence of the functionalization step.

The membranes were tested in a single-module H_2-fed fuel cell and showed good barrier properties towards the fuel cross over. The analysis of the polarization curves revealed a good activity towards O_2 reduction (i_0 ~ 12 μA cm^{-2} with 0.5 mg cm^{-2} of Pt loading), confirmed by the kinetic parameters derived by the best fitting procedure of the EIS spectra.

The best performances were reached by functionalizing the membrane for 24 h with a promising power density peak of ~ 370 mW cm^{-2} using 1 mg cm^{-2} as Pt loading at the electrodes, maintained even after cell shut down and restart.

The slope of the ohmic region provides a resistance value higher than that measured with CS/phosphotungstic acid suggesting that there are still options to optimize the synthesis conditions for enhancing the fuel cell performance.

Acknowledgements Dr. Irene Gatto (CNR ITAE Institute for Advanced Energy Technologies "N. Giordano", Italy) is gratefully acknowledged for providing Pt electrodes.

References

1. Wang Y, Chen KS, Mishler J, Cho SC, Adroher XC (2011) A review of polymer electrolyte membrane fuel cells: technology, applications, and needs on fundamental research. Appl Energy 88:981–1007
2. Dicks AL, Rand DAJ (2018) Fuel cell systems explained. Wiley, Chichester, UK
3. Mauritz KA, Moore RB (2004) State of understanding of nafion. Chem Rev 104:4535–4586
4. Peighambardoust SJ, Rowshanzamir S, Amjadi M (2010) Review of the proton exchange membranes for fuel cell applications. Int J Hydrogen Energy 35:9349–9384
5. Zhang L, Chae S-R, Hendren Z, Park J-S, Wiesner MR (2012) Recent advances in proton exchange membranes for fuel cell applications. Chem Eng J 204–206:87–97
6. Tripathi BP, Shahi VK (2011) Organic–inorganic nanocomposite polymer electrolyte membranes for fuel cell applications. Prog Polym Sci 36:945–979
7. Inamuddin D, Mohammad A, Asiri AM (2017) Organic–inorganic composite polymer electrolyte membranes. Springer International Publishing, Cham
8. Kabir MDL, Kim HJ, Choi S-J (2017) Comparison of several acidified Chitosan/Nafion® composite membranes for fuel cell applications. J Nanosci Nanotechnol 17:8128–8131
9. Rinaudo M (2006) Chitin and chitosan: properties and applications. Prog Polym Sci 31:603–632
10. Kourasi M, Wills RGA, Shah AA, Walsh FC (2014) Heteropolyacids for fuel cell applications. Electrochim Acta 127:454–466
11. Santamaria M, Pecoraro CM, Di Quarto F, Bocchetta P (2015) Chitosan–phosphotungstic acid complex as membranes for low temperature H_2–O_2 fuel cell. J Power Sources 276:189–194
12. Pecoraro CM, Santamaria M, Bocchetta P, Di Quarto F (2015) Influence of synthesis conditions on the performance of chitosan–heteropolyacid complexes as membranes for low temperature H_2–O_2 fuel cell. Int J Hydrogen Energy 40:14616–14626
13. Santamaria M, Pecoraro CM, Di Franco F, Di Quarto F, Gatto I, Saccà A (2016) Improvement in the performance of low temperature H_2–O_2 fuel cell with chitosan–phosphotungstic acid composite membranes. Int J Hydrogen Energy 41:5389–5395
14. Santamaria M, Pecoraro CM, Di Franco F, Di Quarto F (2017) Phosphomolybdic acid and mixed phosphotungstic/phosphomolybdic acid chitosan membranes as polymer electrolyte for H_2/O_2 fuel cells. Int J Hydrogen Energy 42:6211–6219
15. Cui Z, Xing W, Liu C, Liao J, Zhang H (2009) Chitosan/heteropolyacid composite membranes for direct methanol fuel cell. J Power Sources 188:24–29
16. Deivanayagam P, Jaisankar SN (2012) Synthesis and characterization of composite membranes derived from mono sulfonated poly (ether sulfone) and silicotungstic acid. J Macromol Sci A 49:1092–1098

17. Vijayalekshmi V, Khastgir D (2018) Fabrication and comprehensive investigation of physicochemical and electrochemical properties of chitosan-silica supported silicotungstic acid nanocomposite membranes for fuel cell applications. Energy 142:313–330
18. Deivanayagam P, Sivasubramanian G, Hariharasubramanian K, Baskar B, Gurusamy Thangavelu SA (2019) Energy material—the role of silicotungstic acid and fly ash in sulfonated poly (ether sulfone) composites for PEMFC applications. J Macromol Sci A 56:146–152
19. Brooker RP, Baker P, Kunz HR, Bonville LJ, Parnas R (2009) Effects of silicotungstic acid addition to the electrodes of polymer electrolyte membrane fuel cells. J Electrochem Soc 156:B1317–B1321
20. Mason KS, Neyerlin KC, Kuo M-C, Horning KC, More KL, Herring AM (2012) Investigation of a silicotungstic acid functionalized carbon on Pt activity and durability for the oxygen reduction reaction. J Electrochem Soc 159:F871–F879
21. Baker PS, Bonville LJ, Russell Kunz H (2014) Performance of silicotungstic acid modified platinum cathodes at high temperature and low relative humidity for PEMFCs. J Electrochem Soc 161:F1307–F1313
22. Gatto I, Saccà A, Carbone A, Pedicini R, Urbani F, Passalacqua E (2007) CO-tolerant electrodes developed with phosphomolybdic acid for polymer electrolyte fuel cell (PEFCs) application. J Power Sources 171:540–545
23. Cervera MF, Heinämäki J, Räsänen M, Maunu SL, Karjalainen M, Acosta OMN, Colarte AI, Yliruusi J (2004) Solid-state characterization of chitosans derived from lobster chitin. Carbohydr Polym 58:401–408
24. Zhang W, Zhang J, Jiang Q, Xia W (2012) Physicochemical and structural characteristics of chitosan nanopowders prepared by ultrafine milling. Carbohydr Polym 87:309–313
25. Wan Y, Creber KAM, Peppley B, Tam Bui V (2004) Ionic conductivity and tensile properties of hydroxyethyl and hydroxypropyl chitosan membranes. J Polym Sci B 42:1379–1397
26. Songsiri N, Rempel GL, Prasassarakich P (2017) Liquid-phase synthesis of isoprene from MTBE and formalin using cesium salts of silicotungstic acid. Mol Catal 439:41–49
27. Narayanaswamy Venkatesan P, Dharmalingam S (2017) Characterization and performance study of phase inversed sulfonated poly ether ether ketone—silico tungstic composite membrane as an electrolyte for microbial fuel cell applications. Renew Energy 102:77–86
28. Cui Z, Xiang Y, Si J, Yang M, Zhang Q, Zhang T (2008) Ionic interactions between sulfuric acid and chitosan membranes. Carbohydr Polym 73:111–116
29. Chen G-Y, Wang C, Lei Y-J, Zhang J, Mao Z, Mao Z-Q, Guo J-W, Li J, Ouyang M (2017) Gradient design of Pt/C ratio and Nafion content in cathode catalyst layer of PEMFCs. Int J Hydrogen Energy 42:29960–29965
30. Wlodarczyk R, Kolary-Zurowska A, Marassi R, Chojak M, Kulesza PJ (2007) Enhancement of oxygen reduction by incorporation of heteropolytungstate into the electrocatalytic ink of carbon supported platinum nanoparticles. Electrochim Acta 52:3958–3964
31. Thanganathan U (2016) Synthesis and characterization of hybrid composite membranes and their properties: single cell performances based on carbon black catalyst/proton-conducting hybrid composite membrane for H_2/O_2 fuel cells. J Memb Sci 517:100–110

Publisher's Note Springer Nature remains neutral with regard to jurisdictional claims in published maps and institutional affiliations.